

Wide angle phase only Computer Generated Hologram by Angular Spectrum Compact Space Bandwidth Product method

Artur Szawerdak, Dawid Ciesielski, Tomasz Kozacki*

Faculty of Mechatronics, Warsaw University of Technology, 8 Św. A. Boboli St. 75, 02-525 Warszawa

Received December 23, 2025; accepted February 19, 2026; published March 31, 2026

Abstract—Wide-angle capability is critical for holographic near-eye displays. Since most systems employ phase-only spatial light modulators (SLMs), computer-generated holograms (CGHs) must be encoded as phase-only holograms (PoHs). This work presents two approaches for PoH-based CGH generation from plane images: a direct single-step method (D-PoH) and an iterative method (I-PoH). Both utilize the Compact Space-Bandwidth Angular Spectrum (CSW-AS) technique for propagation, which is optimal for wide-angle scenarios. We evaluate their accuracy and zero-padding requirements. Results show that I-PoH provides a higher quality image, but at the cost of cyclic computations and the requirement of substantially larger zero-padding compared to D-PoH, limiting its efficiency for wide-angle applications. In contrast, I-PoH achieves a maximum field of view (FoV) of 39°, while D-PoH enables a significantly larger FoV of 54°, for a PC with 64GB RAM. These findings demonstrate the advantage of direct single-step encoding for achieving wide-angle holographic displays.

Holographic displays are widely regarded as one of the most promising technologies for eyewear applications, particularly in holographic head-up displays (HNEDs). Unlike stereoscopic or light-field techniques, holography reproduces three-dimensional scenes with accurate focus cues, thereby eliminating the conflict between convergence and accommodation. This advantage stems from the principle of diffraction governing the reconstruction of images from encoded holograms. HNED display 3D content directly to the observer's eyes. The human visual system requires a field of view (FoV) of approx. 60° for central vision and up to 120° for peripheral vision. This coverage requires pixel sizes well below a micron and high-quality images with very high resolution. In practice, holographic images are digitally synthesized using computer-generated holography (CGH), which encodes the object as a complex amplitude or phase signal. The hologram is reconstructed by modulating light on a spatial light modulator (SLM), typically only in phase. Therefore, the CGH must be encoded as a pure phase hologram (PoH).

The straightforward approach is to take the object wave and propagate it into a hologram and encode it as a complex amplitude signal CGH using single-step methods. These methods include double phase hologram (DPH) [1] and complex amplitude modulation (CAM) [2]. However, these methods significantly limit the field of view for wide-angle (WA) displays. The simple approach, known as the direct PoH encoding method, involves taking the phase from the CGH. This method does not limit the field of view, but it provides lower image quality [3].

State-of-the-art approaches often employ calculations based on cyclic diffraction [4–5]. Among these, iterative algorithms such as the Gerchberg-Saxton (GS) method are widely used due to their ability to obtain high-fidelity images with minimal noise; however, this advantage comes at the cost of high computational overhead. The most advanced and promising PoH CGH utilize learning architectures, enabling fast task execution while achieving high-quality reconstructions. Nevertheless, approaches based on cyclic diffraction calculations remain impractical for WA display applications because they require fast diffraction calculations that are not currently available.

Propagation algorithms are essential components of iterative PoH (I-PoH) and single-step D-PoH layer-based methods. However, WA scenarios pose significant challenges for these algorithms, primarily because they impose extremely high memory requirements that are often impossible to satisfy. Publication [6] proposes the Multi Fast Fourier Transform Angular Spectrum (MFFT-AS) method, which improves calculations for larger angles by applying tiling operations. However, in MFFT-AS, the sample size at input and output is equal; thus, for larger angles, the method becomes too expensive.

Reconstruction methods based on the Compact Space-Bandwidth Angular Spectrum (CSW-AS) technique use a larger output sampling size. This reduces the signal space bandwidth product [7] and enables the reconstruction of an extended FoV. Nevertheless, due to the discrete nature of calculations, especially when pixel sizes are smaller than 1 μm , the reconstructed wavefield is susceptible to aliasing errors. These problems can be mitigated by using zero-padding in the spatial and frequency domain [7]. However, the volume of zero-padding depends on pixel size, propagation distance, and configuration. As a result, calculations become too demanding for pixel sizes smaller than 0.8 μm . The recent paper proposed an alternative, namely the Non-Uniform Fourier Domain Stretching (NU-FDS) method [8], which is based on the Fourier Transform, Fresnel diffraction, and non-uniform magnification. NU-FDS can reconstruct the CGH as up to 16K and a FoV of up to 120°. However, only forward propagation is possible; thus, the method cannot be used for PoH CGH.

Currently, no WA CGH algorithm exists for input data represented as a single 2D image or a stack of 2D slices.

* E-mail: tomasz.kozacki@pw.edu.pl



This is due to WA HNED geometry, where the object is at a large distance from the observer, as required by the geometry, and from the AS propagator, where the pixel size remains constant in both the object and observation planes. Consequently, the achievable field of view becomes narrow. Moreover, the recently introduced carrier-frequency multiplexing technique [9] also employs an AS propagator extending FoV for this data type, providing a noticeable improvement; however, the achievable FoV is relatively small. Thus, this paper develops two WA PoH CGH methods, namely D-PoH and I-PoH, that utilize the CSW-AS propagator, as it offers the best computational capabilities for this WA application.

The D-PoH method begins by taking the input object image and adding a random phase distribution to improve information transfer efficiency. The combined complex field is then propagated to the hologram plane using the CSW-AS propagator, and the resulting hologram is encoded as a pure phase hologram by extracting only the phase component, which can be written as:

$$U = \exp \{i\angle[S^- [A \exp\{i\varphi_{rand}\}]]\}, \quad (1)$$

where φ_{rand} are random numbers between 0 to 2π , A is the image amplitude, U is a hologram and $S^{\pm}[\cdot]$ are forward and backward CSW-AS operators, respectively.

The I-PoH method, in turn, performs iterative optimization using a relaxation parameter β as:

$$U'_n = S^+ [\exp\{i\angle U_n\}], \quad (2)$$

$$U_{n+1} = S^- [(1 - \beta)U'_n + \beta A \exp\{i\angle U'_n\}], \quad (3)$$

for forward and backward direction, where U_n , U'_n is the calculated field at the hologram and image plane, respectively. This technique reduces to the conventional GS algorithm for the special case of $\beta=1$. The proposed I-PoH is similar to the Successive Over-Relaxation technique [10] that apply an overestimation to the solution using a so-called relaxation parameter β .

These methods enable WA CGH generation for flat 2D objects, a type of data previously unsupported under WA conditions and representing the first step toward layer-based algorithms. The CSW-AS limitations regarding the minimum supported pixel pitch size for WA CGH geometry are investigated, revealing key computational trade-offs. While D-PoH offers superior efficiency, I-PoH requires more iterations and significantly larger zero-padding, making it less memory-efficient but yielding substantially higher reconstruction quality.

To assess the performance of the CSW-AS algorithm, we consider two representative geometrical configurations. The evaluation involves reconstructing two holograms generated via the point-source technique of Ref. [11]. Two 4K holograms (4096×4096 pixels, $\lambda=0.5\mu\text{m}$) were synthesized for an object placed at 0.5m and comprising three rectangles: the largest spanning 90% of the FoV, and the other two occupying 60% and 30% of the FoV, respectively. These holograms at the $z=0.5\text{m}$ provide

image spaces of sizes $0.17 \times 0.17\text{m}^2$ (FoV=19°) and $0.35 \times 0.35\text{m}^2$ (FoV=39°). Reconstructions were performed using CSW-AS under two conditions: without zero-padding and with space-frequency zero-padding (zero-padding applied in both space and frequency domains). The results are presented in Fig. 1, where the left column corresponds to a pixel pitch of $1.5\mu\text{m}$ and the right column to a pixel pitch of $0.75\mu\text{m}$. The upper panels depict reconstructions with zero-padding, while the lower panels show those without. The findings clearly indicate that zero-padding is indispensable for mitigating aliasing artifacts. Nevertheless, the computational overhead of zero-padding is substantial, increasing the data size to 4670×4670 for $1.5\mu\text{m}$ and to 26974×26974 for $0.75\mu\text{m}$. In the first case, the size of the zero padding was calculated according to Ref. [7]. However, in the second case, the computed value of zero-padding providing data size of 11240×11240 was insufficient because aliasing in the corners; therefore, an additional 140% zero padding was applied. The amount of zero padding is examined later in this paper and is presented in Fig. 4f. This computational overhead becomes prohibitive for smaller pixel pitches, effectively limiting the applicability of CSW-AS.

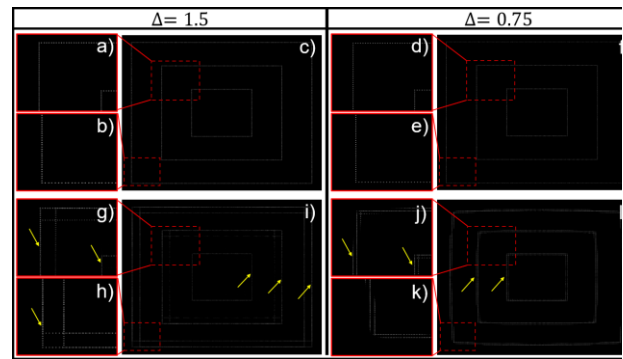


Fig. 1 CSW-AS reconstruction of 4K CGHs (left: $\Delta=1.5\mu\text{m}$; right: $\Delta=0.75\mu\text{m}$). With zero-padding (a-b) and without (c-d). Each subfigure includes zoomed-in fragments, highlighting reconstruction accuracy differences. Arrows indicate correctly reconstructed rectangles.

Next, we illustrate the performance of the D-PoH and I-PoH algorithms, which utilize the AS-CSW propagator with the zero-padding conditions discussed above. For both pixel pitches of $1.5\mu\text{m}$ and $0.75\mu\text{m}$, 4K D-PoH holograms were synthesized. In this case, the object was a planar image of a camera man. The holograms were reconstructed using the NU-FDS method, and the results are presented in Fig. 2. The reconstructions accurately represent the object; however, noticeable noise is present, although aliasing artifacts are not observed. For both D-PoH CGHs, the zero-padding amount was determined according to Ref. [7], which, for pixel $0.75\mu\text{m}$ is 7144×7144 , and it is considerably smaller than 22878×22878 , which is necessary to guarantee accurate reconstruction in Fig. 1b. Thus, interestingly, for D-PoH CGH, even with substantially reduced zero padding,

aliasing does not disturb the image. To demonstrate the aliasing-free CGH generations, all images in Fig. 2 show reconstructions obtained using the NU-FDS method.

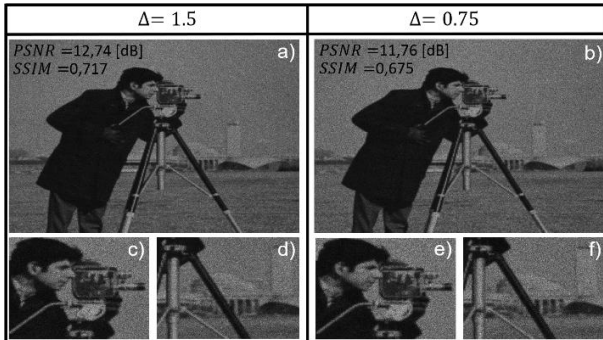


Fig. 2 Numerical reconstruction of D-PoHs obtained via NU-FDS.

This paper also proposes an iterative WA I-PoH method with CSW-AS propagator and relaxation parameter β . In our experiment, 4K CGHs were generated with a ten-iteration algorithm. For the first four iterations $\beta=1$ (GS algorithm), while for the next six $\beta=2$. Figure 3 illustrates the algorithm's performance for the zero-padding parameters applied within the D-PoH framework and calculated according to Ref. [7], whose corresponding output is presented in Fig. 2. For a pixel pitch of $1.5\mu\text{m}$, the algorithm achieves alias-free results with improved image quality. Conversely, when the pixel size is reduced to $0.75\mu\text{m}$, noticeable aliasing artifacts appear in the image corners. The obtained aliasing is visible in the reconstruction presented in Fig. 3f calculated via NU-FDS. It is worth noting the absence of aliasing in Fig. 3b. This phenomenon can be explained by iteratively encoded aliasing in the image. Since the image content is encoded in the corner aliasing areas, its reconstruction in Fig. 3f using the NU-FDS propagation method shows errors.

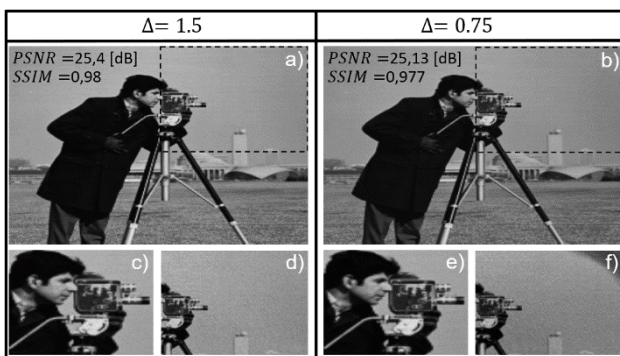


Fig. 3 Numerical reconstruction of I-PoHs obtained via CSW-AS (a, b, c, e) and NU-FDS (d, f) for zero-padding of Ref. [7].

The aliasing observed in Fig. 3f is because, in the study of Ref. [7], the aliasing analysis was conducted for a point located at the midpoint of the image edge rather than at the corner. To properly account for corner points, additional zero-padding is required, which in this case amounts to 22878×22878 . Consequently, for a hologram with a pixel size of $0.75\mu\text{m}$, the reconstruction was

performed using this larger zero-padding. The resulting output, shown in Fig. 4, demonstrates high-quality reconstruction without aliasing artifacts. Furthermore, Fig. 4d illustrates the zero-padding requirements for both D-PoH and I-PoH, highlighting that the requirements for I-PoH are substantially higher, particularly at smaller pixel sizes. Additionally, it shows that the size of zero-padding is independent of the resolution.

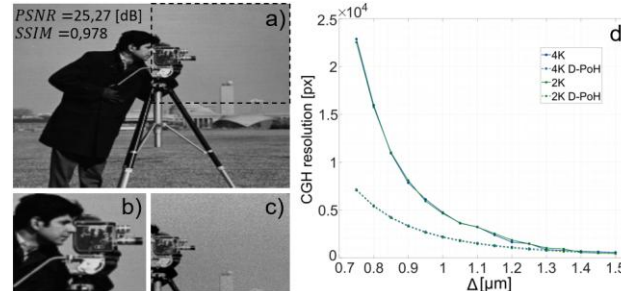


Fig. 4 Numerical reconstruction of I-PoHs obtained via CSW-AS (a–b) and NU-FDS (c) for zero-padding of this work; (d) zero-padding necessary for D-PoH and I-PoH algorithms.

In summary, two methods, D-PoH and I-PoH, were introduced for generating PoH CGHs using CSW-AS propagation. Numerical analysis indicates that for larger pixel sizes, both approaches exhibit comparable zero-padding demands. However, for smaller pixels, D-PoH can successfully generate CGHs even when the CSW-AS propagator introduces aliasing errors, whereas the I-PoH must rely on an aliasing-free CSW-AS algorithm. Thus, I-PoH requires much larger zero padding. Consequently, with D-PoH, we have faster computations: computation time of D-PoH is 9s and I-PoH is 1521s for pixel $0.75\mu\text{m}$, and with D-PoH we can reach FoV up to 54° (impossible for I-PoH, max 39° due to aliasing), while the advantage of I-PoH is achieving superior image quality.

Warsaw University of Technology and National Science Center (2025/07/Y/ST7/00082) funded this research.

References

- [1] O. Mendoza-Yero, G. Mínguez-Vega, J. Lancis, *Opt. Lett.* **39**(7), 1740 (2014).
- [2] Y. Qi, C. Chang, J. Xia, *Opt. Expr.* **24**(26), 30368 (2016).
- [3] A. Szawerdak, R. Kukolowicz, M.S. Idicula, M. Chlipala, T. Kozacki, *Phot. Lett. Poland*, **17**(2), 60 (2025).
- [4] T. Gu, C. Han, H. Qin, K. Sun, *Opt. Expr.* **32**(25), 44358 (2024).
- [5] S.J. Liu, L.F. Feng, S.J. Ji, H.N. Yan, K. Yang, P.P. Li, D. Wang, *Opt. Laser Technol.* **181**, 111644 (2025).
- [6] T. Kozacki, J. Martinez-Carranza, R. Kukolowicz, W. Finke, *Appl. Opt.* **59**, 8450 (2020).
- [7] T. Kozacki, K. Falaggis, *Appl. Opt.* **55**, 5014 (2016).
- [8] T. Kozacki, M.S. Idicula, J. Martinez-Carranza, M. Chlipala, R. Kukolowicz, *Opt. Laser Technol.*, **192**, 113876 (2025).
- [9] S.F. Lin, M.F. Yin, J. Zhao, L. Rong, Y. Wang, D. Wang, *Opt. Laser Technol.* **192**, 113807 (2025).
- [10] G. Strang, *Computational Science and Engineering* (Wellesley-Cambridge Press 2007).
- [11] T. Kozacki, J. Martinez-Carranza, I. Gerej, R. Kukolowicz, M. Chlipala, M.S. Idicula, *Opt. Laser Technol.* **181**, 111610 (2025).